PHYSICAL REVIEW B VOLUME 61, NUMBER 14 1 APRIL 2000-II

Temperature dependent changes of the Mn 3*d* and 4*p* bands near T_c in colossal magnetoresistance systems: XANES study of $La_{1-x}Ca_xMnO_3$

F. Bridges
Department of Physics, University of California, Santa Cruz, California 95064

C. H. Booth and G. H. Kwei
Los Alamos National Laboratory, Los Alamos, New Mexico 87545

J. J. Neumeier
Department of Physics, Florida Atlantic University, Boca Raton, Florida 33431

G. A. Sawatzky
Materials Science Center, University of Groningen, 9747 AG Groningen, The Netherlands

(Received 17 May 1999; revised manuscript received 30 December 1999)

We report high-resolution x-ray-absorption near-edge structure measurements at the Mn *K* edge as a function of temperature, for $La_{1-x}Ca_xMnO_3$ samples, with a focus mainly on the pre-edge region. Small peaks labeled A_1–A_3 are observed which correspond to 1*s*-3*d* dipole transitions, made weakly allowed via a hybridization of Mn 4*p* states with Mn 3*d* states on *neighboring* atoms. Adjusting the parameters in a local spin-density approximation calculation to approximately match the experimental A_1-A_2 splitting yields $U=4$ eV and $J_H=0.7$ eV. For colossal magnetoresistance samples, A_1 decreases with T while A_2 increases with T below T_c, which shows that the 3*d* bands change significantly as T moves through T_c. There are also small changes in the shape of the main edge (1*s*-4*p* transitions).

The substituted manganites ($La_{1-x}A_xMnO_3$, where *A* is a divalent metal such as Ca or Sr) exhibit a range of interesting properties[1,2] which depend on interactions between magnetism, charge, and local structure. For concentrations of *A* roughly in the range $0.2 \lesssim x \lesssim 0.48$, these materials have a magnetoresistance which can be very large in thin-film samples[3,4] — hence the name ''colossal'' magnetoresistance (CMR). The CMR materials exhibit a metal-insulator transition near the ferromagnetic transition at the Curie temperature, T_c. The basic mechanism for transport is generally assumed to be governed by double exchange (DE);[5] however, the large size of the observed magnetoresistance (MR) led Millis and co-workers[6–8] to propose that a large lattice distortion may amplify the CMR effect. Recent local-structure measurements[9–15] show that there is a rapid increase in the width of the Mn-O pair-distribution function, σ, as T approaches the ferromagnetic transition temperature. How this distortion interacts with the electronic system, and particularly its impact on the Mn 3*d* bands, is still uncertain. However, it clearly plays a significant role in the polarization dependent hybridization of the 4*p* and 3*d* states.

Several different theoretical models with a variety of parameters have been developed to describe these systems. First a crystal-field splitting (the 10Dq parameter) is expected, which will split the Mn 3*d* levels into a t_{2g} triplet and an e_g doublet.[16] $CaMnO_3$ (Mn^{+4}) has three 3*d* electrons which form a (spin 3/2) local Mn moment with three up spins in the t_{2g} band, while $LaMnO_3$ (Mn^{+3}) has a fourth electron in an e_g state that is Hund-rule coupled to the local Mn moment. An on-site Coulomb repulsion, *U*, typically 4–8 eV for Mn and much larger than the 3*d* bandwidths of order 1–2 eV, strongly suppresses polarity fluctuations of the kind $2Mn^{+3} \rightarrow Mn^{+2} + Mn^{+4}$ resulting in a Mott Hubbard insulating state for the undoped materials. In addition, because Mn^{+3} is a Jahn-Teller (JT) ion, JT distortions are expected (but inversion symmetry is maintained) when Mn^{+3} sites are present, with a JT energy, Δ_{JT}. The position of the broad O band is also important; Pickett and Singh,[17] using the local spin-density approximation (LSDA), suggest that these systems are half-metallic, with a gap between the O band and a minority-spin *d* band. Another early approach assumes a more covalent Mn-O bond;[18–20] here the band at the Fermi surface is a hybridization of the Mn e_g and O 2*p* states. Very recently Elfimov *et al.*[21] have made a more detailed calculation for the $LaMnO_3$ system using LSDA+*U* to understand some recent anomalous diffraction experiments. They include a calculation of the undistorted lattice to understand the influence of the JT splitting.

In this paper we present the pre-edge data (Mn *K* edge) for several different Ca concentrations as a function of temperature. We have used the same data as in a previous study; the reader is referred to Ref. 13 for sample details. The T_c's for the 21 and 30 % samples are 210(2) and 260(2) K, respectively. Additional details about edges will be given in a more comprehensive paper.[22]

In Fig. 1 we show the Mn *K* edge for several samples using Si 220 monochromator crystals (resolution ~0.4 eV). In each case the main edge is sharp and has a long, low-energy tail. The main edge is attributed to transitions to Mn 4*p* states (1*s*-4*p*) which lie *far above* the Fermi energy, E_F, and hence its position does not correspond to E_F, which is in the lower e_g band. Although the density of states is large for

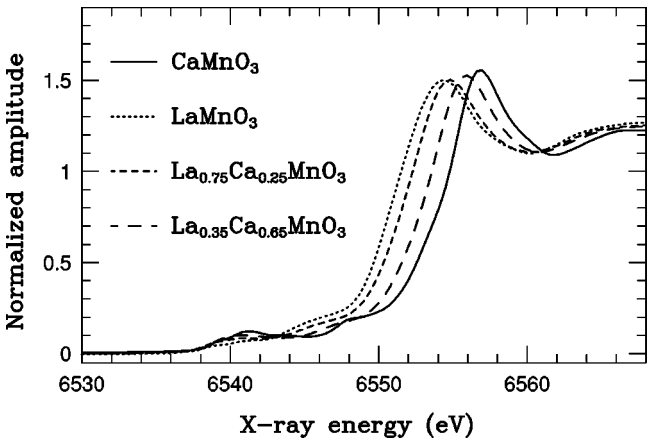

FIG. 1. The Mn K edges for several Ca concentrations. The absolute edge energies are determined by the energy of the first inflection point of a Mn-foil reference sample. We have set this inflection point at 6537.4 eV for Mn (Ref. 14).

the empty e_g bands, they are not directly accessible via dipole transitions. Thus the main K-edge absorption begins where the large part of the $4p$ density of states (DOS) occurs; it determines roughly where the zero of kinetic energy occurs (as is assumed in most x-ray-absorption fine-structure analyses). The shape of this edge is remarkably similar to the calculations by Elfimov *et al.*[21] of the Mn $4p$ partial density of states, broadened by the known core-hole lifetime. (See Fig. 2 in their paper.) The calculations also indicate a low-energy tail, with small features far below the main edge which correspond well to the A and B peaks discussed in more detail below. They also show that the $4p$ DOS is very broad; consequently, the Mn $4p$ states are highly delocalized and extend over several Mn atoms. A similar broad Mn $4p$ DOS in these systems has also been obtained by Benfatto *et al.* for $LaMnO_3$ using multiple-scattering theory.[23]

The low intensity pre-edge region, which extends roughly from 6535 to 6550 eV, is presented in Figs. 2 and 3. At room temperature the A_2 peak position is nearly constant for all Ca concentrations at 6541.2 ± 0.2 eV, while the A_1 position shifts slightly upward with increasing Mn valence (i.e., increasing x). As a result, the separation between the A_1 and A_2 peaks is largest for $LaMnO_3$, at 2.2 eV. These results are very similar to earlier observations on other Mn oxides,[24,25] including the increase of the A-peak amplitude with Mn valence.[24,26] In general such transitions are weakly allowed either through the quadrupole interaction or via hybridization of the Mn $3d$ states with p states; for the Mn oxide materials, it has been suggested that the latter dominates.[24] These previous studies have not focused on magnetic systems, and have not considered the possibilities of large U or Hund's rule coupling, J_H. Consequently, the A_1 peak was assigned to transitions into empty t_{2g} states and A_2 transitions into e_g states with the splitting given by the crystal-field-splitting, 10Dq. In view of the high spin state for Mn in the manganites this cannot be correct, and an alternative interpretation will be presented here. Another feature, which we label the B peak, occurs at the top of this range, and is also associated with Mn $4p$ states.[24]

For $LaMnO_3$ and $La_{0.35}Ca_{0.65}MnO_3$ the peak amplitudes, A_i, have a weak temperature dependence below 300 K.

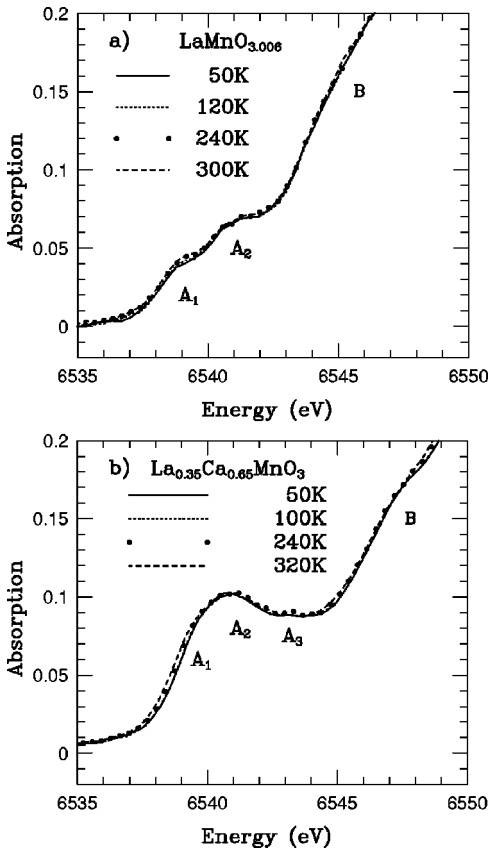

FIG. 2. The weak temperature dependence of the pre-edge region for the $LaMnO_3$ and 65% Ca samples; these data change very little up to 300 K. A_3, near 6543 eV, becomes more prominent for $CaMnO_3$.

However for CMR samples, these peaks have an unusual temperature dependence, as shown in Fig. 3 for 21 and 30 % Ca. The A_1 peak decreases with temperature while A_2 increases as T is increased through T_c. In addition, the A_2 peak shifts slightly downward by 0.3 to 0.5 eV for $T < T_c$. This is very unusual as the A_2 position is generally constant for a range of materials.[24] This dependence is shown in more detail for the 21% sample in Fig. 4, where the difference between the data at temperature T and the data at 300 K is plotted. (Note that each trace must first be corrected for any energy shift of the beamline using the Mn powder reference data.) The increase for A_1 occurs primarily over a small range of temperatures ($\sim$60 K) below $T_c \sim 210$ K. The difference for A_2 is negative over the same temperature range, but the change is smaller in magnitude. No significant change within the signal-to-noise (S/N) ratio is observed between 200 and 300 K for the A_i peaks. In addition, there are clear systematic changes in the shape of the main edge ($1s$-$4p$ transitions). Relative to the 50 K data, the lower part of the edge at 300 K has a slight increase (near 6551 eV) while the upper part has a corresponding small decrease (near 6553), which is suggestive that at high T there are two distinct Mn sites with slightly different valence states. However, the situation is complicated and will be addressed more fully in a longer paper.[22]

The $1s$-$3d$ transitions are often described in terms of $3d^{n+1}$ final states, where n is the initial number of $3d$ electrons; $n=3$ for $CaMnO_3$ and $n=4$ for $LaMnO_3$. However,

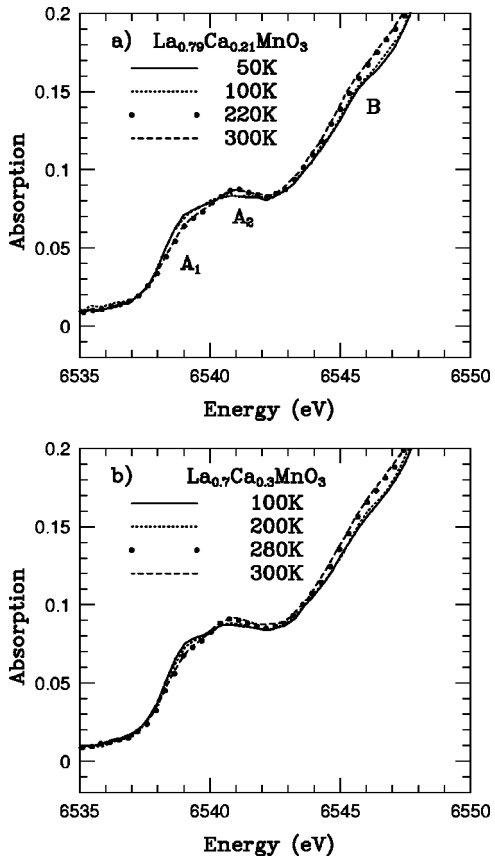

FIG. 3. The temperature dependence of the pre-edge region for the CMR samples (21 and 30 % Ca) up to 300 K. These samples have a similar temperature dependence as T increases through T_c. The A_1, A_2, and B peaks are indicated in panel (a).

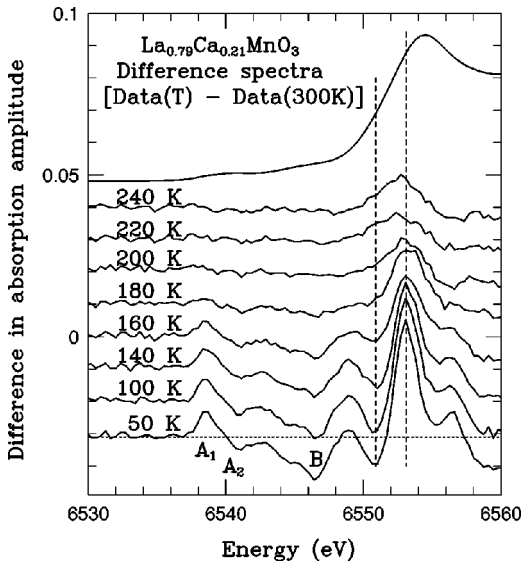

FIG. 4. A plot of the difference between the data collected at temperature T and 300 K for the 21% Ca sample. Most of the change occurs over a 60 K temperature range below T_c ($T_c \sim 210$ K); note that there is essentially no change above 200 K. The full edge, multiplied by a factor 0.03 to fit this scale, is shown at the top. The pre-edge peaks A_1, etc., have the largest relative change; the changes in the main edge are a few percent of the step height.

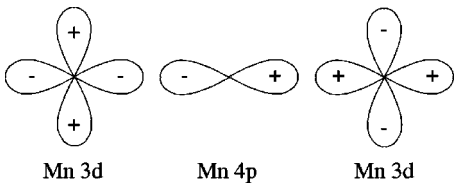

FIG. 5. A schematic arrangement of the neighboring Mn 3*d* orbitals that would have ungerade symmetry about the central Mn atom. This linear combination will hybridize with the Mn 4*p* state.

the interpretation of the *A* peaks depends on the model used to describe the system, and for the manganites, the hybridization of *p* and *d* states also appears to be a crucial ingredient. In addition, the explanation for the intensity of these peaks as arising from *p*-*d* mixing on the excited atom is also unsatisfactory because the Mn atom is at a point of inversion symmetry for the cubic Mn oxides and $CaMnO_3$, and nearly so even for substituted $LaMnO_3$. A very important point about this problem emerges from the calculation of Elfimov[21] — the 3*d* features correspond to a coupling of the Mn 4*p* states with 3*d* states on *adjacent* Mn atoms. The explanation is based on symmetry and band-structure arguments. For the central core excited Mn atom at a center of inversion symmetry, the 4*p* states centered on this atom cannot directly hybridize with its own 3*d* states[27] because these have even parity for inversion. However the central Mn 4*p* orbitals can hybridize with a linear combination of neighboring O 2*p* orbitals which have odd parity. They can also couple, via the O, with a linear combination of Mn 3*d* orbitals centered on more distant Mn ions. For example a linear combination of Mn 3*d* orbitals can be formed with odd symmetry as illustrated in Fig. 5. Here we do not include the O 2*p* orbitals between the Mn ions via which the main part of the hybridization proceeds.

Using the new calculations[21] as a guide, A_1 would correspond to transitions into empty majority-spin e_g states on the neighboring Mn ions and A_2 to transitions into the e_g and t_{2g} minority states. The initial calculations, using $U=8$ eV and $J_H=0.88$ eV (per spin pair)[21] yielded an A_1-A_2 splitting close to 3 eV which is considerably larger than the experimental value of 2.2 eV for $LaMnO_3$. Revised calculations with more realistic values, $U=4$ eV and $J_H=0.7$ eV, result in a splitting of about 2 eV, close to the experimental value. Very roughly one would expect this splitting to be given by $4J_H=2.8$ eV since in the final state the Mn *d* occupation is 5*d* electrons. The smaller splitting found in these band-structure calculations is due to a difference in hybridization of the minority and majority-spin bands, causing a breakdown of this simple estimation; for the smaller parameters, there is an increase in covalency with holes in the O band. For $CaMnO_3$ we would again expect in the simple approximation, a splitting roughly $J_H=0.7$ eV smaller. The experimental decrease of the A_1-A_2 splitting (0.3–0.5 eV, $LaMnO_3$ to $CaMnO_3$) is considerably smaller, perhaps again because of the oversimplified nature of the estimate. A LSDA+U calculation for $CaMnO_3$ would shed some light on this discrepancy. One should keep in mind here that the Ca compound is expected to be considerably more covalent because of the higher oxidation state of Mn. This increased covalency would reduce the effective J_H because the spins are actually

delocalized over Mn and the neighboring O ions. In the actual band-structure calculations this effect is included.

Understanding the observed temperature dependence of the A peaks will require a better theoretical understanding of the role of hybridization and its dependence on the spin-spin, orbital-orbital, and charge-charge correlation functions between neighboring ions. It is these correlation functions which obviously change as we go through the magnetic phase transition. For example, we expect the spin-polarized band widths to change in a manner consistent with the double exchange arguments for the CMR materials. Also, changes in the overlap between the $4p$ states and the surrounding O and Mn states are very sensitive to interatomic distances and therefore strongly affect the intensities of the transitions, especially the pre-edge features.

In summary, we have introduced an interpretation of the pre-edge features as arising from a hybridization of the Mn $4p$ states with $3d$ states on neighboring Mn atoms. In terms of recent theoretical calculations, the A_1 and A_2 are transitions into majority e_g states and minority e_g and t_{2g} states, respectively. To fit the experimental splitting, smaller values of U and J_H are required than in the initial calculations.[21] Because the intensity of these features is strongly dependent on hybridization and local distortions, the observed temperature dependence of the pre-edge may be an interesting probe of hybridization in these materials.

We thank S. Satpathy and D. Dessau for helpful conversations. This work was conducted under NSF Grant No. DMR-9705117. The experiments were performed at SSRL, which is operated by the DOE, Division of Chemical Sciences, and by the NIH, Biomedical Resource Technology Program, Division of Research Resources.

[1] G. H. Jonker and J. H. van Santen, Physica (Amsterdam) **16**, 337 (1950).
[2] P. Schiffer, A. Ramirez, W. Bao, and S-W. Cheong, Phys. Rev. Lett. **75**, 3336 (1995).
[3] S. Jin *et al.*, Science **264**, 413 (1994).
[4] R. M. Kusters *et al.*, Physica B **155**, 362 (1989).
[5] C. Zener, Phys. Rev. **82**, 403 (1951).
[6] A. J. Millis, B. I. Shraiman, and R. Mueller, Phys. Rev. Lett. **77**, 175 (1996).
[7] A. J. Millis, Phys. Rev. B **53**, 8434 (1996).
[8] A. J. Millis, R. Mueller, and B. I. Shraiman, Phys. Rev. B **54**, 5405 (1996).
[9] S. J. L. Billinge *et al.*, Phys. Rev. Lett. **77**, 715 (1996).
[10] C. H. Booth, F. Bridges, G. J. Snyder, and T. H. Geballe, Phys. Rev. B **54**, R15 606 (1996).
[11] D. Louca *et al.*, Phys. Rev. B **56**, R8475 (1997).
[12] C. H. Booth *et al.*, Phys. Rev. Lett. **80**, 853 (1998).
[13] C. H. Booth *et al.*, Phys. Rev. B **57**, 10 440 (1998).
[14] G. Subías, J. García, M. G. Proietti, and J. Blasco, Phys. Rev. B **56**, 8183 (1997).
[15] G. Subías, J. García, J. Blasco, and M. G. Proietti, Phys. Rev. B **57**, 748 (1998).
[16] S. Satpathy, Z. S. Popović, and F. R. Vukajlović, Phys. Rev. Lett. **76**, 960 (1996).
[17] W. E. Pickett and D. J. Singh, Phys. Rev. B **53**, 1146 (1996).
[18] J. Zaanen, G. A. Sawatzky, and J. W. Allen, Phys. Rev. Lett. **55**, 418 (1985).
[19] J. Zaanen and G. A. Sawatzky, Phys. Rev. B **33**, 8074 (1986).
[20] A. E. Bocquet *et al.*, Phys. Rev. B **46**, 3771 (1992).
[21] I. S. Elfimov, V. I. Anisimov, and G. A. Sawatzky, Phys. Rev. Lett. **82**, 4264 (1999).
[22] F. Bridges *et al.* (unpublished).
[23] M. Benfatto, Y. Joly, and C. R. Natoli, Phys. Rev. Lett. **83**, 636 (1999).
[24] A. Manceau, A. I. Gorshkov, and V. A. Drits, Am. Mineral. **77**, 1133 (1992).
[25] M. Belli *et al.*, Solid State Commun. **35**, 355 (1980).
[26] M. Croft *et al.*, Phys. Rev. B **55**, 8726 (1997).
[27] C. Brouder, J. Phys.: Condens. Matter **2**, 701 (1990).